Journal of Statistical Physics, Vol. 47, Nos. 3/4, 1987

Fractal Boundary of Domain of Analyticity of the Feigenbaum Function and Relation to the Mandelbrot Set

Michael Nauenberg[1]

Received August 14, 1986

The universal map for the period-doubling transition to chaos is studied numerically in the complex plane. The boundary of the domain of analyticity of this function is obtained graphically and is shown to be a fractal with self-similar properties obtained by rescaling with the universal constants α and δ. In the complex parameter plane, this domain is shown asymptotically to be similar to part of the Mandelbrot set.

KEY WORDS: Feigenbaum function; Mandelbrot set.

1. INTRODUCTION

The analyticity properties of the Feigenbaum–Cvitanovic fixed-point function $g(z)$ for the period-doubling bifurcation transition to chaos[1,2] have been studied by Epstein and Lascoux,[3] who have shown that $g(z)$ is analytic in a domain with a natural boundary. The function $g(z)$ is the solution of the functional equation

$$g(z) = -\alpha g(g(z/\alpha)) \tag{1}$$

where $g(z)$ is normalized to $g(0)=1$, with $g'(0)=0$ and $g''(0)<0$, and $\alpha = 2.5029...$ is a universal scaling constant determined self-consistently by this equation. A proof of the existence of a solution of Eq. (1) was first given by Lanford[4] and Campanimo and Epstein.[5]

In this paper, we study numerically the solution of an extended functional equation

$$g(z, \varepsilon) = -\alpha g(g(z/\alpha, \varepsilon/\delta), \varepsilon/\delta) \tag{2}$$

[1] Department of Physics, University of California, Santa Cruz, California 95064.

0022-4715/87/0500-0459$05.00/0

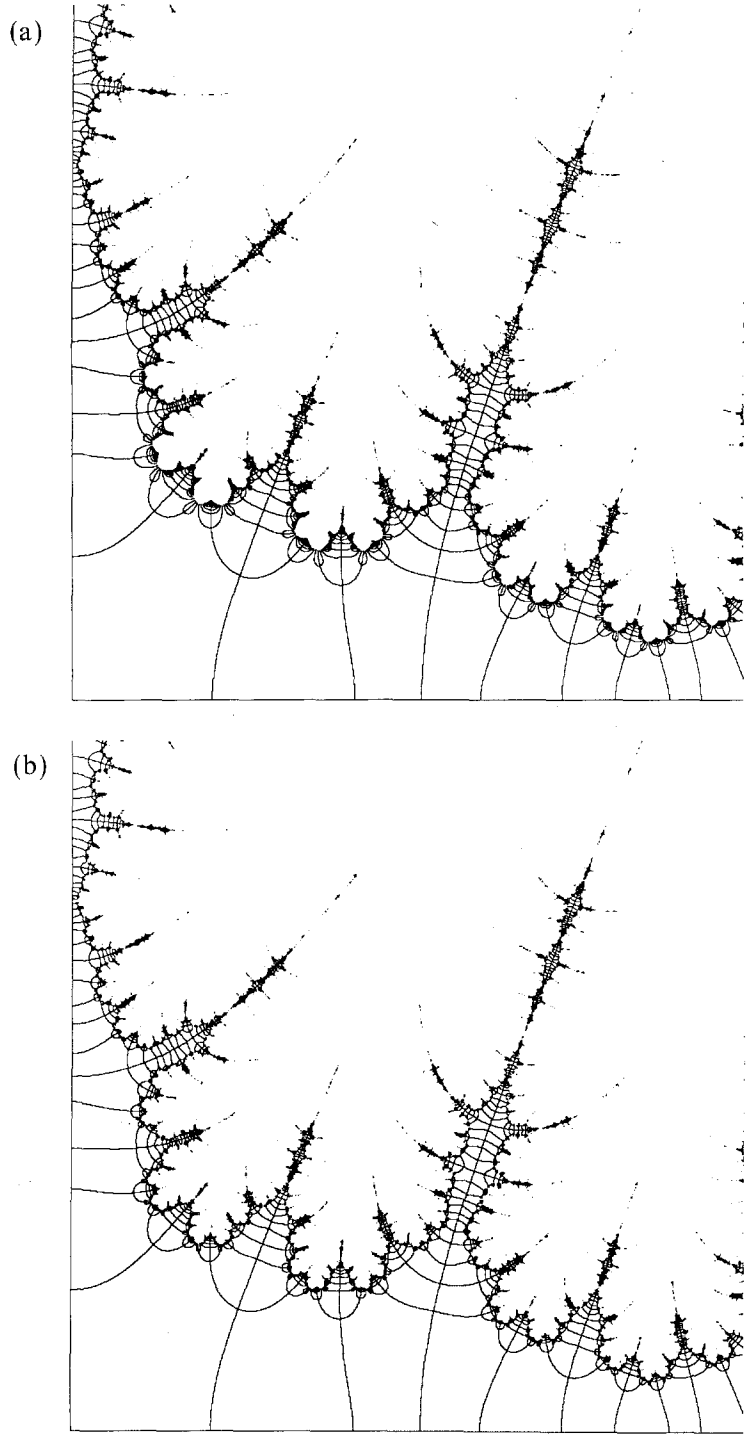

Fig. 1. Contours in the complex z plane for $\mathrm{Im}\, g_n(z)=0$ in the range $0 \leqslant x \leqslant 10$ and $0 \leqslant y \leqslant 10$ for (a) $n=6$, (b) $n=7$.

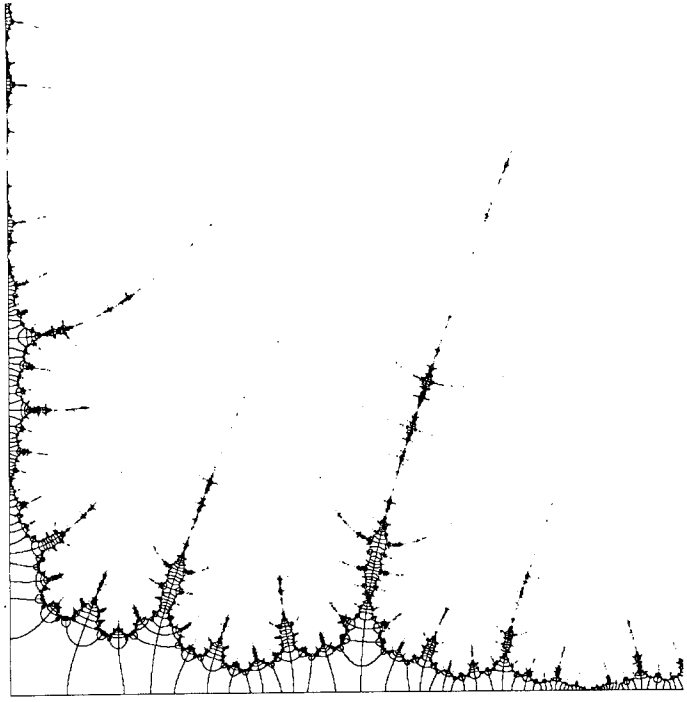

Fig. 2. Contours in the complex z plane for $\operatorname{Im} g_n(z)=0$ in the range $0<x<10\alpha$ and $0<y<10\alpha$ for $n=6$.

where $\delta=4.6692...$ is the universal constant associated with rescaling in the complex ε parameter space. This functional equation is the renormalization-group transformation for period doubling in the space of functions $g(z, \varepsilon)$, where $g(z, 0)=g(z)$ is the fixed point. A similar equation was considered originally[1] to first order in ε, leading to a linear operator that determines the single relevant eigenvalue δ. We shall be interested here in evaluating the domain in the complex z and ε plane, where there exists a solution of this functional equation; this is also the domain of analyticity of $g(z, \varepsilon)$. In particular, for $z=0$ we will show the relation of this domain to the well-known Mandelbrot set[6] in the neighborhood of the critical point $\varepsilon=0$.

The functional equation (2) can be solved by introducing a sequence of polynomials $g_n(z, \varepsilon)$

$$g_n(z, \varepsilon)=(-\alpha)^n f^{(2^n)}(z/\alpha^n, \varepsilon/\delta^n) \tag{3}$$

for $n = 1, 2,...,$ where $f^{(m)}(z, \varepsilon) = f(f,..., f(z, \varepsilon), \varepsilon)$ is the mth iterate of the quadratic map

$$f(z, \varepsilon) = 1 - (c + \varepsilon) z^2 \tag{4}$$

and $c = 1.401155...$ is the critical value for period-doubling bifurcations. It can be readily shown that any sequence of functions defined by Eq. (3) for a general map $f(z, \varepsilon)$ satisfies the functional relation

$$g_{n+1}(z, \varepsilon) = -\alpha g_n(g_n(z/\alpha, \varepsilon/\delta), \varepsilon/\delta) \tag{5}$$

for arbitrary values of α and δ. However, when α and δ are the universal scaling constants and $f(z, \varepsilon)$ is the quadratic map, Eq. (4), we show numerically that the sequence of polynomials $g_n(z, \varepsilon)$ converges uniformly provided that z and ε are restricted to values inside a complex domain. By a theorem in complex variables, there exists a function $g(z, \varepsilon)$ analytic inside this domain that is the limit of the sequence $g_n(z, \varepsilon)$. According to

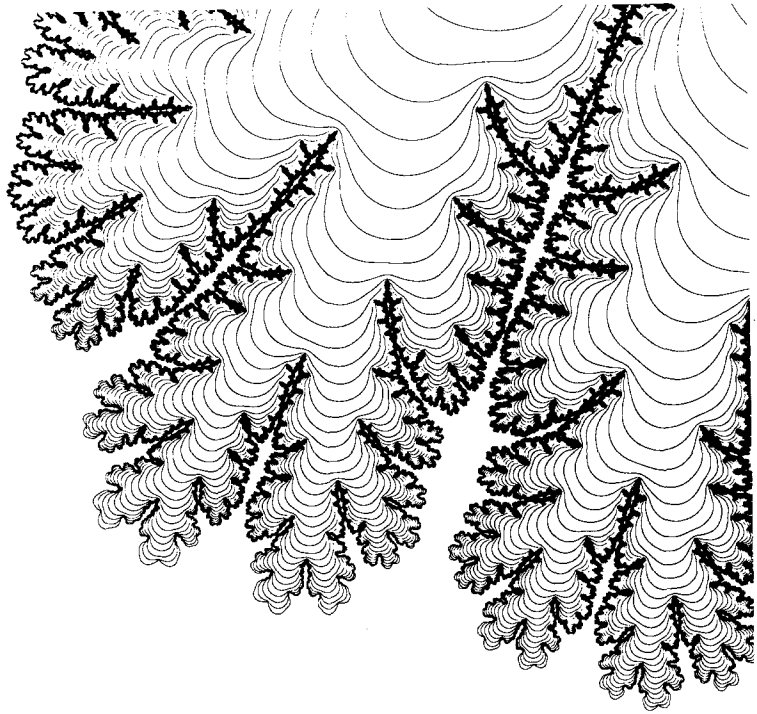

Fig. 3. Contours in the complex z plane when m changes by unity, where m is the number of iterations for which $|f^{(m)}(z/\zeta^n)| > 10^6$, and $n = 6$.

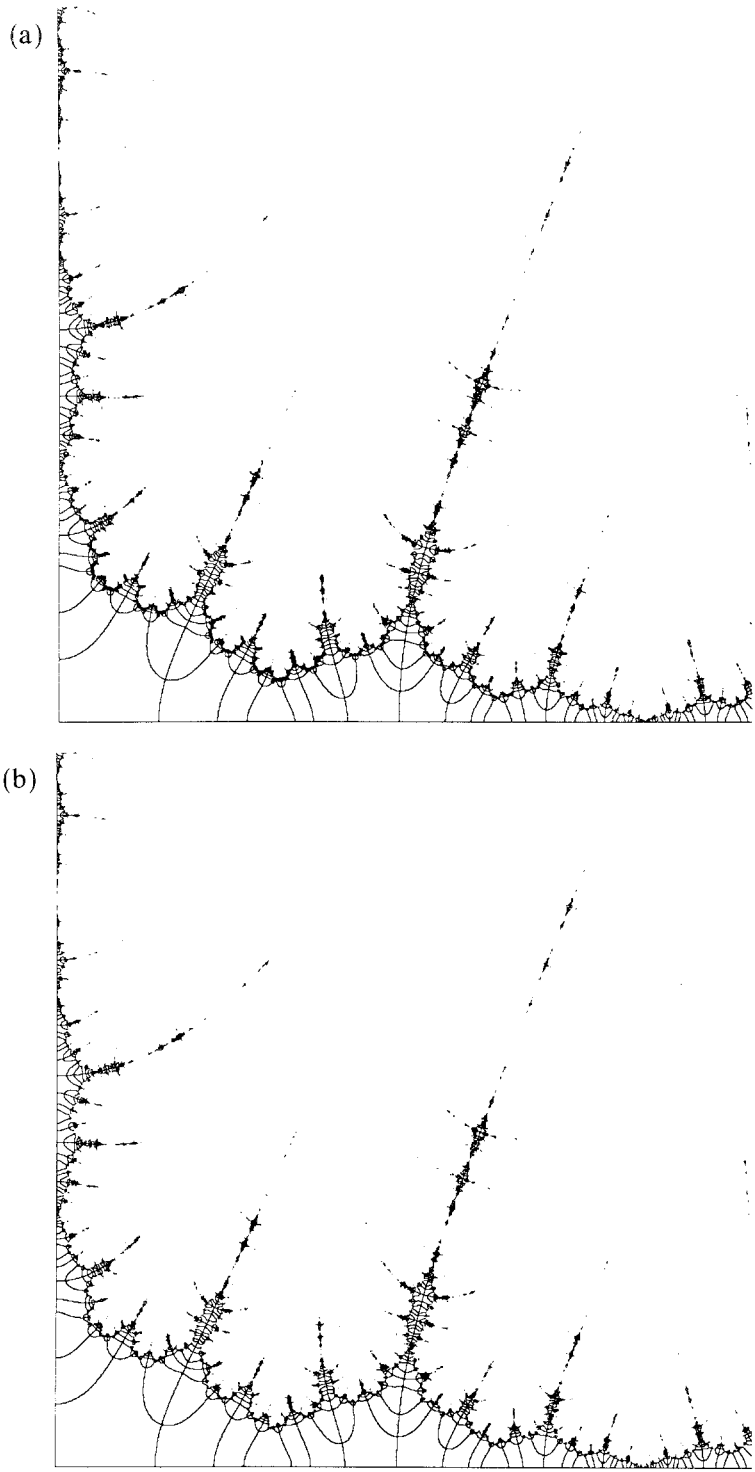

Fig. 4. Contours in the complex z plane for Im $g_n(z, \varepsilon) = 0$ in the range $0 < x < 10\alpha$ and $0 < y < 10\alpha$ for $\varepsilon = -0.01\delta^5$ and (a) $n = 6$, (b) $n = 7$.

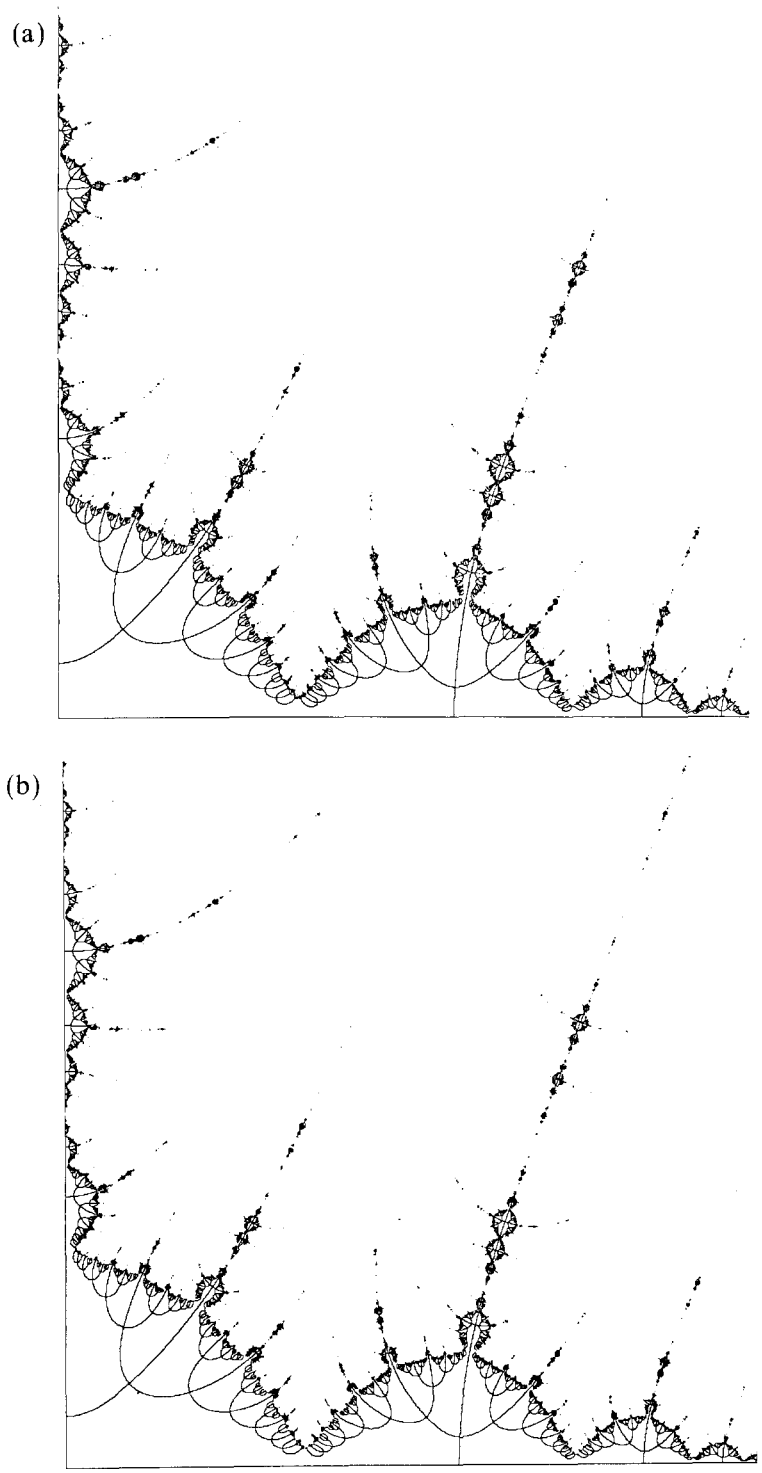

Fig. 5. Contours in the complex z plane for Im $g_n(z, \varepsilon) = 0$ in the range $0 < x < 50$ and $0 < y < 0$ for $\varepsilon = -0.1\delta^5$ and (a) $n = 6$, (b) $n = 7$.

Eq. (5), $g(z, \varepsilon)$ is therefore a solution of our functional equation (2). Expanding $g(z, \varepsilon)$ in a Taylor series in ε and substituting in Eq. (2), it can be shown that $g(z, \varepsilon)$ is the unique solution of Eq. (2) apart from an overall scaling constant. For values of z and ε outside of this domain we find that the absolute value of $g_n(z, \varepsilon)$ increases without bounds as n increases. This implies that $g(z, \varepsilon)$ is analytic in a domain with a natural boundary, as was by Epstein and Lascoux[3] for the special case that $\varepsilon = 0$. We show by several graphical examples that this boundary is a fractal with self-similar properties under rescaling by the universal constants α and δ. In particular, the domain of analyticity of $g(0, \varepsilon)$ in the complex ε plane is similar to part of the Mandelbrot set,[6] defined by the complex values of ε for which

$$\lim_{m \to \infty} |f^{(m)}(0, \varepsilon)| < \infty \tag{6}$$

This connection accounts for the observed approximate self-similarity of the Mandelbrot set under a rescaling by the factor δ near $\varepsilon = 0$, and

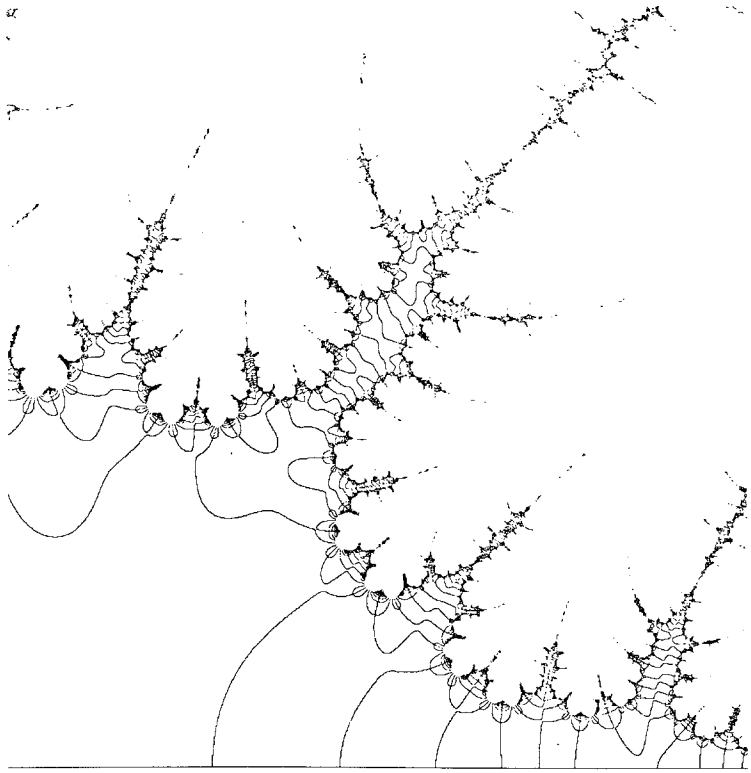

Fig. 6. Contours in the complex ε plane for Im $g_n(0, \varepsilon) = 0$ in the range $-50 < \text{Re}\,\varepsilon < 50$ and $0 < \text{Im}\,\varepsilon < 100$, for $n = 6$.

likewise of the associated Julia sets, which are approximately self-similar under rescaling by a factor α. In connection with the Mandelbrot set, general functional equations for period n-tuplings have been developed recently,[7-10] with $n=2$ corresponding to Eq. (2). We expect that our discussion, which is confined to period doubling, can be readily extended to the more general case.

2. GRAPHICAL RESULTS

A convenient way to represent graphically the complex functions $g_n(z, \varepsilon)$, Eq. (3), is to plot contours of constant values of its real and imaginary parts. We start with the Feigenbaum fixed-point function $g(z)$, and show in Figs. 1a and 1b the contours in the complex $z=x+iy$ plane for Im $g_n(z)=0$ in the range $0 \leqslant x \leqslant 10$ and $0 \leqslant y \leqslant 10$ for $n=6$ and $n=7$, respectively. The solutions are restricted to the upper right-hand quadrant, because $g_n(-z)=g_n(z)$ and $g_n^*(z)=g_n(z^*)$. These contours are terminated whenever $|g_n(z)|>r$, where we have chosen $r=10^6$, but the graphical results are insensitive to the choice of a large upper bound for $|g_n(z)|$. A careful comparison of the contours in these two figures demonstrates graphically the rapid convergence of the sequence $g_n(z, \varepsilon)$ inside the domain of validity of Eq. (2), as well as the fractal nature of the boundary of this domain, which appears with increasing resolution as n increases.

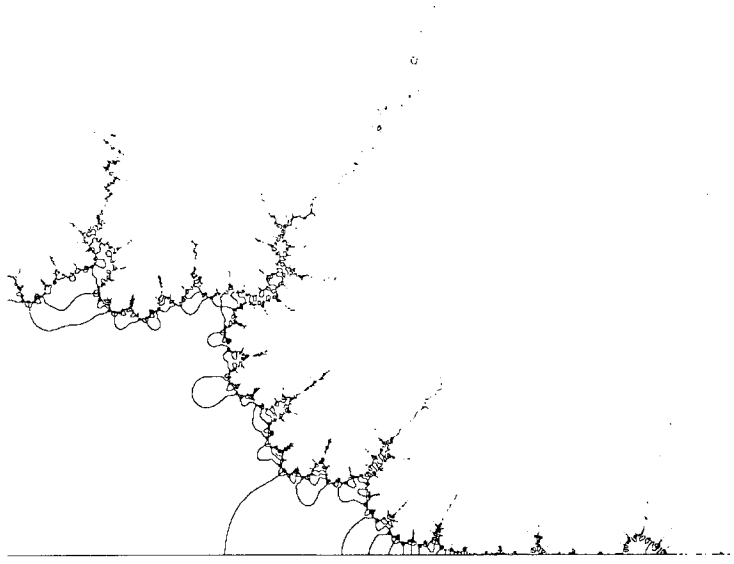

Fig. 7. Contours in the complex ε plane for Im $g_n(0, \varepsilon)=0$ in the range $-50\delta < \text{Re}\,\varepsilon < 50\delta$ and $0 < \text{Im}\,\varepsilon < 100\delta$, for $n=6$.

The scaling of the domain of analyticity, which follows from Eq. (1), is illustrated in Fig. 2 by showing the same contours in the range $0 < x < 10\alpha$ and $0 < y < 10\alpha$. A picture of a few contours for Im $g(z) = 0$ near $z = 0$ was obtained originally by Epstein and Lascoux.[3]

The complement of this domain can be evaluated numerically by determining the complex values of z for which the absolute value of the mth iterate $f^{(m)}(z/\alpha^n, 0)$ exceeds some large upper bound. This is shown in Fig. 3: the contours separate regions where the number of iterations m, with $m < 2^n$, differs by one. Since $|z| = \infty$ is an attractor for the quadratic map, Eq. (4), the fractal boundary of this domain is also approximately the scaled Julia set associated with this map at the critical point. This connection implies that the domain of analyticity of $g(z)$ cannot be extended beyond this boundary, as has been shown rigorously in Ref. 3.

The fractal boundary is the location of the singularities of $g(z)$. It has been shown[3,4] that the singularities that lie nearest to the origin are determined by the condition

$$g(z_0/\alpha) = z_0^* \tag{7}$$

where z_0 is determined numerically; $z_0 = \pm 1.83126 \pm i2.68317$. It can be readily seen that Eq. (1) implies that inside the domain of analyticity near $z = z_0$, $g(z)$ has the power-law form

$$g(z) \cong c/(z - z_0)^p \tag{8}$$

where the exponent $p = \ln \alpha / \ln(\beta/\alpha)$, and $g'(z_0/\alpha) = \beta\varepsilon^{i\phi}$. Numerically we

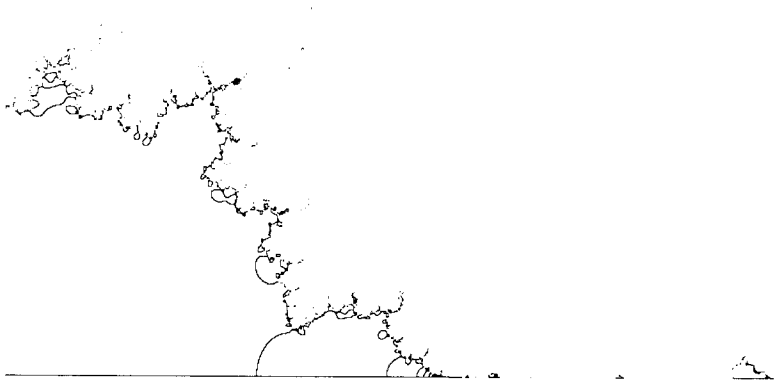

Fig. 8. Contours in the complex ε plane for Im $g_n(0, \varepsilon) = 0$ in the range $-50\delta^2 < \text{Re}\,\varepsilon < 50\delta^2$ and $0 < \text{Im}\,\varepsilon < 100\delta^2$, for $n = 6$.

find that $\beta = 4.924931$ and $\phi = 0.8621162$, which gives $p = 1.355446$. The residue c is a function of z satisfying the condition

$$c^*(z^* - z_0^*) = -e^{ip\phi} c[g'(z_0/\alpha)(z - z_0)/\alpha] \tag{9}$$

but we find numerically that c is approximately a constant.

To illustrate the dependence of $g(z, \varepsilon)$ on ε and the convergence of the sequence $g_n(z, \varepsilon)$, we show, as an example, in Figs. 4a and 4b, the contours for Im $g_n(z, \varepsilon) = 0$ with $\varepsilon = -0.01\delta^5$, for $n = 6$ and 7, respectively, and in Figs. 5a and 5b the corresponding contours for $\varepsilon = -0.1\delta^5$. The contours

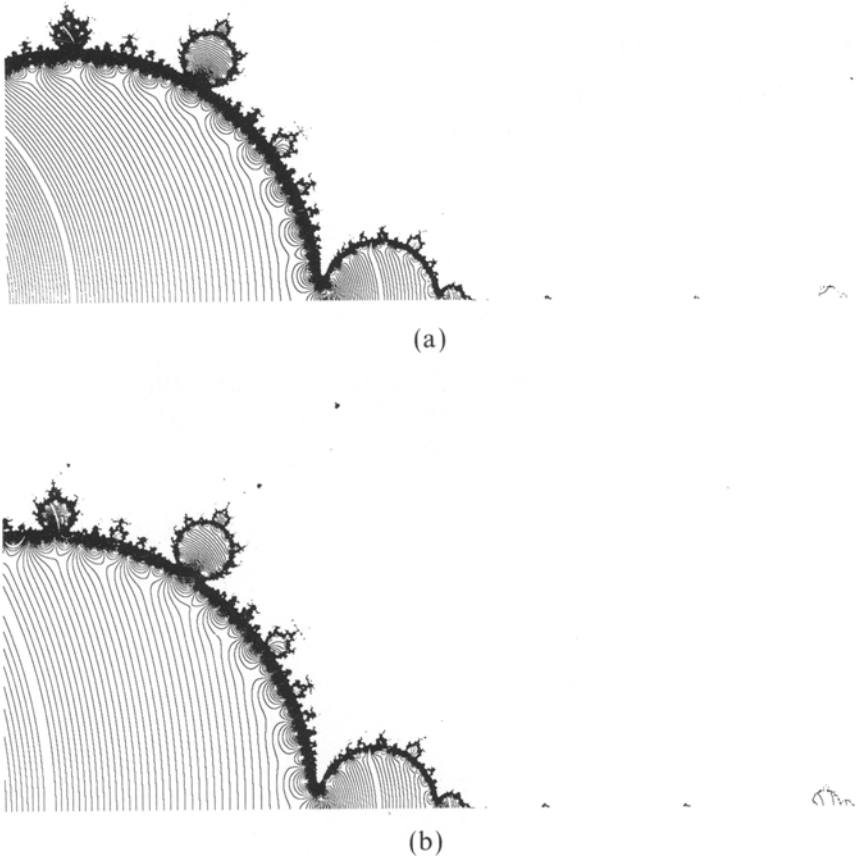

Fig. 9. Contours in the complex ε plane for constant values of real $g_n(0, \varepsilon)$ in the range $-0.1\delta^7 < \mathrm{Re}\,\varepsilon < 0.1\delta^7$ and $0 < \mathrm{Im}\,\varepsilon < 0.2\delta^7$ for (a) $n = 6$, (b) $n = 7$.

for different n are indistinguishable except along the tips of the antennae-like regions, which grow as n increases. We shall return to this point later.

Next we consider the domain of analyticity of $g(z, \varepsilon)$ for $z = 0$ in the complex ε plane. In Fig. 6, we show the contours $\operatorname{Im} g_n(0, \varepsilon) = 0$ for $n = 6$ in the range $-50 < \operatorname{Re} \varepsilon < 50$ and $0 < \operatorname{Im} \varepsilon < 100$. The fractal structure of the boundary of this domain has remarkable similarities with the corresponding fractal boundary of the domain of analyticity of $g(z)$ in the complex z plane. Figures 7 and 8 show the corresponding domain scaled up by a factor δ and δ^2, respectively, illustrating the appearance of the boundary of a Mandelbrot-like set. This connection is shown more clearly in Figs. 9a and 9b, where we plot contours of constant values of the real part

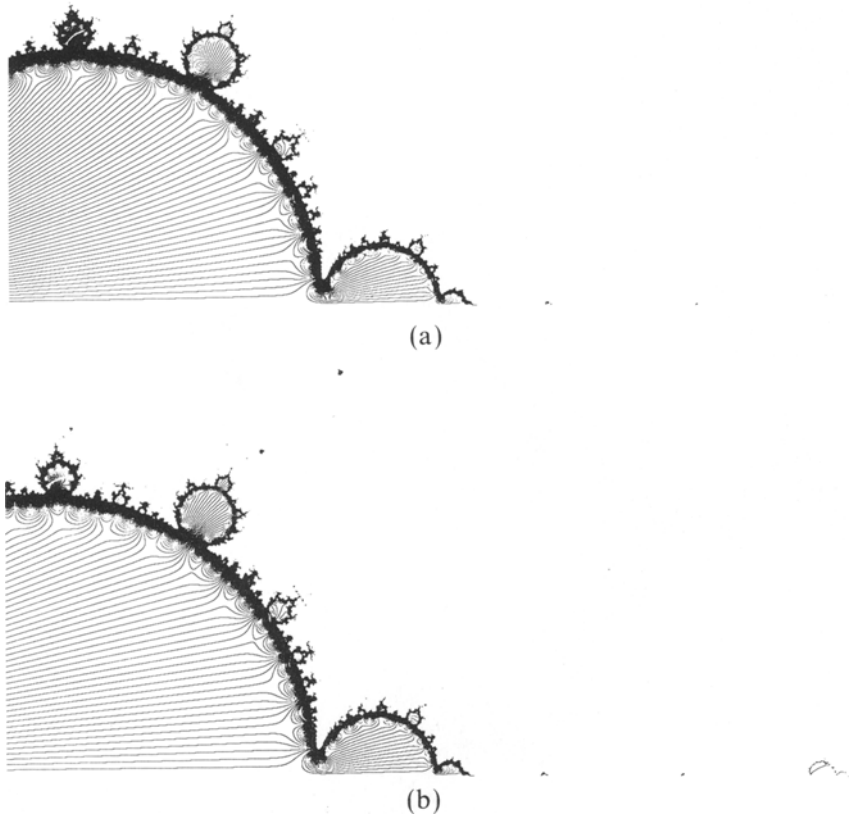

Fig. 10. Contours in the complex ε plane for constant values of $\operatorname{Im} g_n(0, \varepsilon)$ in the range $-0.1\delta^7 < \operatorname{Re} \varepsilon < 0.1\delta^7$ and $0 < \operatorname{Im} \varepsilon < 0.2\delta^7$ for (a) $n = 6$, (b) $n = 7$.

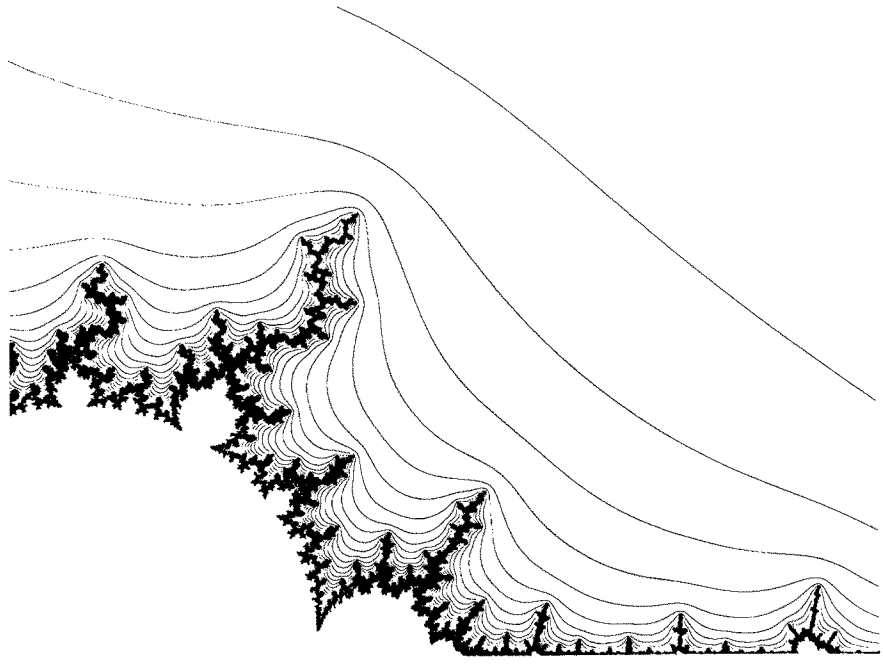

(a)

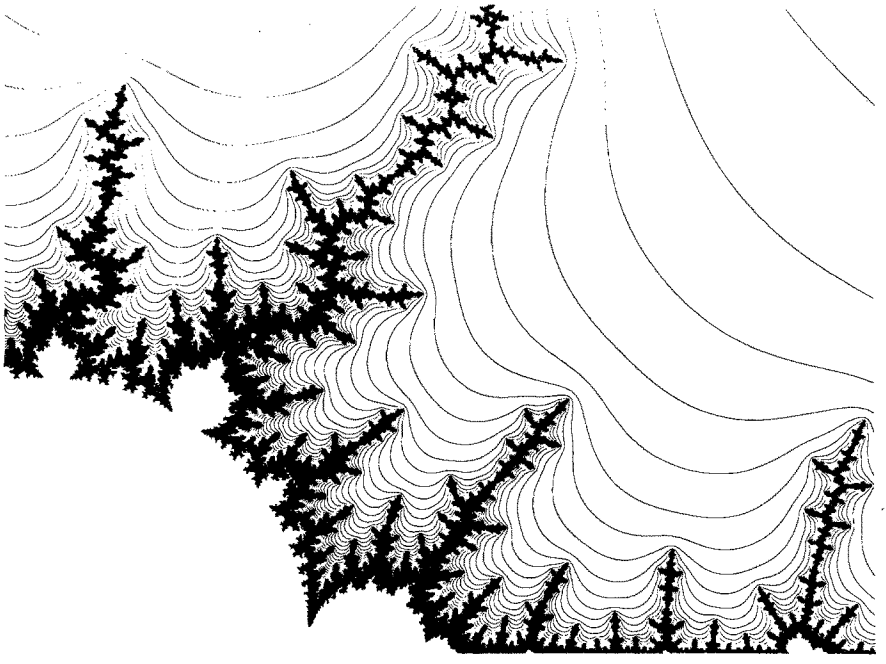

(b)

Fig. 11. Contour in the complex ε plane when m changes by unity, where m is the number of iterations such that $|f^m(0, \varepsilon/\delta^n)| > 10^6$ with $-0.1\delta^7 < \mathrm{Re}\,\varepsilon < 0.1\delta^7$ and $0 < \mathrm{Im}\,\varepsilon < 0.2\delta^7$ and (a) $n = 6$, (b) $n = 7$.

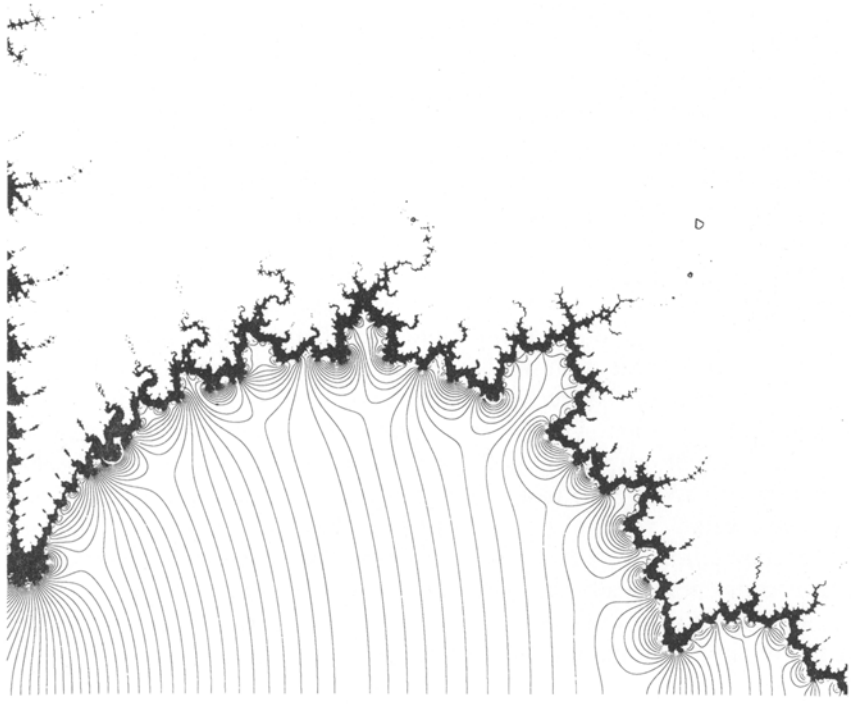

(a)

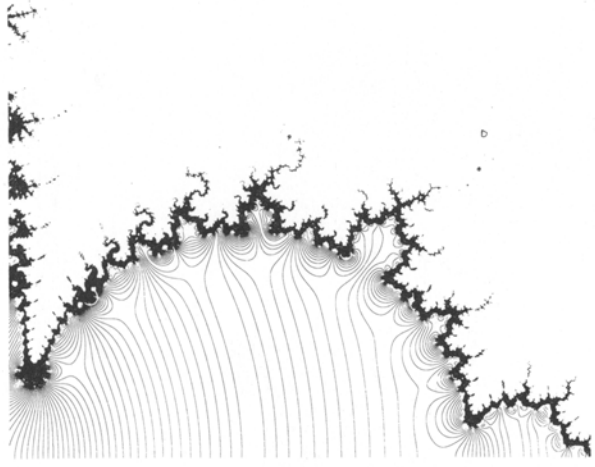

(b)

Fig. 12. Contours in the complex ε plane for constant values of real $g_n(0, \varepsilon)$ in the range $-0.1\delta^6 < \mathrm{Re}\,\varepsilon < 0$ and $0 < \mathrm{Im}\,\varepsilon < 0.2\delta^7$ for (a) $n = 6$, (b) $n = 7$.

of $g_n(0, \varepsilon)$ for $n=6$ and 7, respectively, in the range $-0.1\delta^7 < \mathrm{Re}\,\varepsilon < 0.1\delta^7$ and $0 < \mathrm{Im}\,\varepsilon < 0.2\delta^7$, and in Figs. 10a and 10b, where we plot the corresponding contours for the imaginary part of $g_n(0, \varepsilon)$. The complement of this set is shown in Figs. 11a and 11b, where we evaluate the number of iterates m for which $|f^m(0, \varepsilon/\delta^n)| > 10^6$ for $n=6$ and 7, and plot contours where m changes by unity, for $m < 2^n$. This is also a graphical method for evaluating the complement of the Mandelbrot set, but only approximately, because, according to Eq. (6), there should be no restrictions on the number of iterations m. Note that the rapid accumulation of these contours into treelike structures does not appear in Figs. 9 and 10 except for some dark specks, which correspond to the white specks inside the trees of Fig. 11. Blowups of these specks show that these regions are also Mandelbrot-like sets. The absence of the treelike structures in Figs. 9 and 10 is due to lack of graphical resolution. This is demonstrated, for example, in Figs. 12a and 12b, which are blowups of Figs. 9a and 9b, and in Fig. 6, where the treelike structures are resolved. Figure 12 also resolves in further detail the contours of constant value of real $g_n(0, \varepsilon)$ near the fractal boundary, showing the accumulation of these contours near the fractal boundary; this demonstrates graphically that $g(0, \varepsilon)$ is singular on this boundary.

The convergence of $g_n(0, \varepsilon)$ is verified numerically by comparing corresponding contours for different values of n. In particular, it is evident

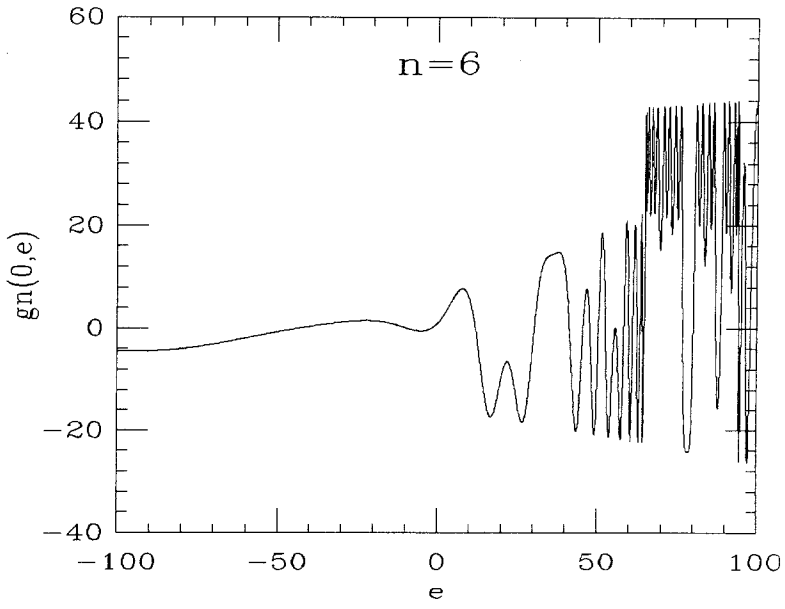

Fig. 13. The function $g_n(0, \varepsilon)$ for $\mathrm{Im}\,\varepsilon = 0$ in the interval $-100 \leqslant \mathrm{Re}\,\varepsilon \leqslant 100$ and $n=6$.

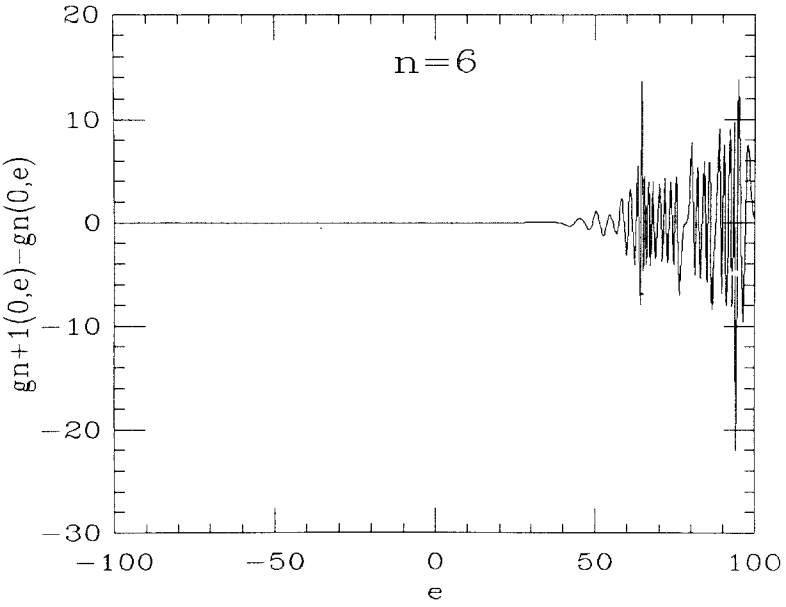

Fig. 14. The difference $g_{n+1}(0, \varepsilon) - g_n(0, \varepsilon)$ for $\operatorname{Im} \varepsilon = 0$ in the interval $-100 < \operatorname{Re} \varepsilon < 100$ and $n = 6$.

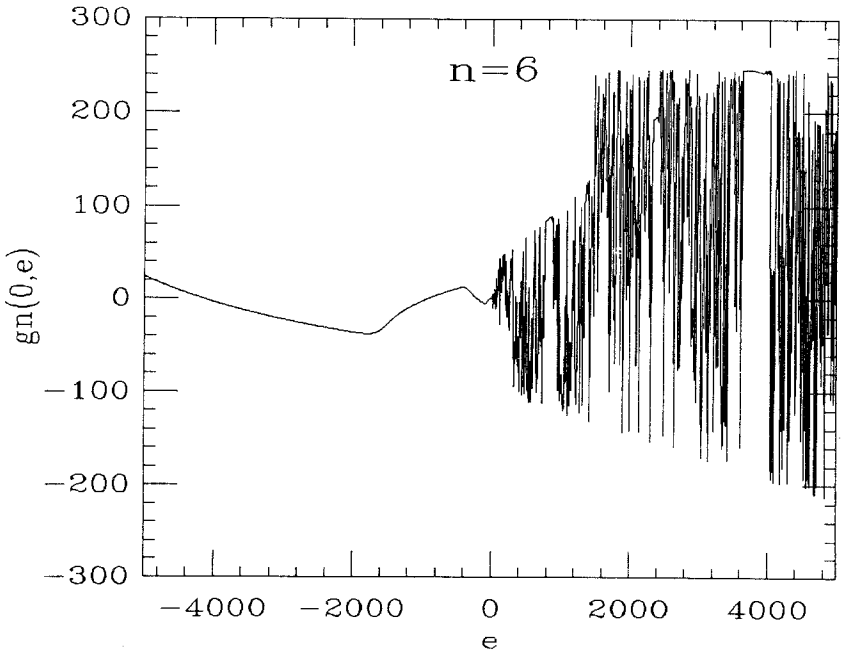

Fig. 15. The function $g_n(0, \varepsilon)$ for $\operatorname{Im} \varepsilon = 0$ in the interval $-4000 < \operatorname{Re} \varepsilon < 4000$ and $n = 6$.

from Figs. 11a and 11b that the treelike regions grow[10] with n, indicating that the convergence is expected to be very slow in these regions. This can be demonstrated along the real ε axis, where we can readily study the behavior of the sequence $g_n(0, \varepsilon)$. In Fig. 13 we plot $g_n(0, \varepsilon)$ for $-100 \leqslant \varepsilon \leqslant 100$ and $n = 6$, showing the onset of rapid oscillations for $e \geqslant 50$, where the domain narrows toward the real axis. Furthermore, the region of rapid oscillation is marked by increasingly slower convergence of the sequence, as can be seen in Fig. 14 where we plot the difference $g_{n+1}(0, \varepsilon) - g_n(0, \varepsilon)$. The amplitude and frequency of these oscillations increase with ε, except for intervals of slow variation, as can be seen in Fig. 15, where we have extended the interval to $-4000 < \varepsilon < 4000$. This interesting behavior is due to the fact that positive, real ε corresponds to the chaotic domain for the quadratic map.

3. SUMMARY

We have shown that the solution $g(z, \varepsilon)$ of the functional equation (2) for the period-doubling transition to chaos is analytic inside a domain in the complex z and ε planes with a fractal boundary that has self-similarity properties under rescaling by the universal constants α and δ. For the fixed-point solution $g(z, 0)$ we have extended the calculation of this domain, which had been studied previously by Epstein and Lascoux.[3] For the function $g(0, \varepsilon)$ the corresponding domain for large values of $|\varepsilon|$ is shown to be similar to part of the Mandelbrot set[6] whose properties have been studied by Douady and Hubbard,[12] Sullivan,[13] and Milnor.[11]

ACKNOWLEDGMENTS

I would like to thank H. O. Peitgen for useful discussions and comments and D. Saupe for advice on graphical techniques.

REFERENCES

1. M. J. Feigenbaum, *J. Stat. Phys.* **19**:25 (1978); **21**:669 (1979); *Los Alamos Science* **1980**:4.
2. P. Coullet and C. Tresser, *C. R. Acad. Sci. Paris* **287A**:577 (1978); *J. Phys. (Paris)* **39**:C5-25 (1978).
3. H. Epstein and J. Lascoux, *Commun. Math. Phys.* **81**:437 (1981).
4. O. E. Lanford III, *Bull. Am. Math. Soc.* **6**:427 (1982).
5. M. Campanimo and H. Epstein, *Commun. Math. Phys.* **79**:261 (1981).
6. B. B. Mandelbrot, in Nonlinear dynamics, R. Helleman, ed., *Ann. N. Y. Acad. Sci.* **357**:249 (1980); *The Fractal Geometry of Nature* (Freeman, San Francisco, 1982); *Physics* **7D**:224 (1983).

7. P. Cvitanovic and J. Myrheim, *Phys. Lett.* **94A**:324 (1983); Nordita preprint (1984).
8. E. B. Vul and D. M. Khanin, *Russ. Math. Surv.* **37**(5):173 (1982).
9. A. I. Golberg, Ya. G. Sinai, and K. M. Khanin, *Russ. Math. Surv.* **38**(1):187 (1983).
10. E. B. Vul, Ya. G. Sinai, and K. M. Khanin, *Russ. Math. Surv.* **39**(3):1 (1984).
11. J. Milnor, Institute for Advance Study preprint (1986).
12. A. Douady and J. H. Hubbard, *C. R. Acad. Sci. Paris* **294**:123 (1982).
13. D. Sullivan, Institute des Hautes Etudes Scientifiques preprints 1982–1983.